

Fabrication of electron beam generated, chirped, phase mask (1070.11–1070.66 nm) for fiber Bragg grating dispersion compensator

R. C. Tiberio, D. W. Carr, M. J. Rooks, S. J. Mihailov, F. Bilodeau, J. Albert, D. Stryckman, D. C. Johnson, K. O. Hill, A. W. McClelland, and B. J. Hughes

Citation: *Journal of Vacuum Science & Technology B* **16**, 3237 (1998); doi: 10.1116/1.590358

View online: <http://dx.doi.org/10.1116/1.590358>

View Table of Contents: <http://scitation.aip.org/content/avs/journal/jvstb/16/6?ver=pdfcov>

Published by the AVS: Science & Technology of Materials, Interfaces, and Processing

Articles you may be interested in


[Highly coherent red-shifted dispersive wave generation around 1.3 \$\mu\$ m for efficient wavelength conversion](#)
J. Appl. Phys. **117**, 103103 (2015); 10.1063/1.4914076

[Robust, efficient grating couplers for planar optical waveguides using no-photoacid generator SU-8 electron beam lithography](#)
J. Vac. Sci. Technol. B **27**, 2602 (2009); 10.1116/1.3258153





[Bandwidth-enhanced volume grating for dense wavelength-division multiplexer using a phase-compensation scheme](#)
Appl. Phys. Lett. **86**, 181103 (2005); 10.1063/1.1921333

[High perfection chirped grating phase masks by electron-beam definition](#)
J. Vac. Sci. Technol. B **17**, 3217 (1999); 10.1116/1.590983

[Electron-beam irradiation-induced nonlinearity in silicate glass films and fabrication of nonlinear optical gratings](#)
J. Appl. Phys. **86**, 2393 (1999); 10.1063/1.371066



Instruments for Advanced Science

<p>Contact Hiden Analytical for further details: W www.HidenAnalytical.com E info@hiden.co.uk</p> <p>CLICK TO VIEW our product catalogue</p>	 <p>Gas Analysis</p> <ul style="list-style-type: none"> › dynamic measurement of reaction gas streams › catalysis and thermal analysis › molecular beam studies › dissolved species probes › fermentation, environmental and ecological studies 	 <p>Surface Science</p> <ul style="list-style-type: none"> › UHV TPD › SIMS › end point detection in ion beam etch › elemental imaging - surface mapping 	 <p>Plasma Diagnostics</p> <ul style="list-style-type: none"> › plasma source characterization › etch and deposition process reaction › kinetic studies › analysis of neutral and radical species 	 <p>Vacuum Analysis</p> <ul style="list-style-type: none"> › partial pressure measurement and control of process gases › reactive sputter process control › vacuum diagnostics › vacuum coating process monitoring
---	--	--	--	--

Fabrication of electron beam generated, chirped, phase mask (1070.11–1070.66 nm) for fiber Bragg grating dispersion compensator

R. C. Tiberio,^{a)} D. W. Carr, and M. J. Rooks^{b)}
Cornell Nanofabrication Facility, Cornell University, Ithaca, New York

S. J. Mihailov, F. Bilodeau, J. Albert, D. Stryckman, D. C. Johnson, and K. O. Hill
Communications Research Centre, Ottawa Ontario, Canada

A. W. McClelland and B. J. Hughes
Leica Lithography Systems, Cambridge, England

(Received 14 September 1998; accepted 17 September 1998)

We report on the fabrication of a chirped, phase mask that was used to create a fiber Bragg grating (FBG) device for the compensation of chromatic dispersion in longhaul optical transmission networks. Electron beam lithography was used to expose the grating onto a resist-coated quartz plate. After etching, this phase mask was used to holographically expose an index grating into the fiber core [K. O. Hill, F. Bilodeau, D. C. Johnson, and J. Albert, *Appl. Phys. Lett.* **62**, 1035 (1993)]. The linear increase in the grating period, “chirp,” is only 0.55 nm over the 10 cm grating. This is too small to be defined by computer aided design and a digital deflection system. Instead, the chirp was incorporated by repeatedly rescaling the analog electronics used for field size calibration. Special attention must be paid to minimize any field stitching and exposure artifacts. This was done by using overlapping fields in a “voting” method. As a result, each grating line is exposed by the accumulation of three overlapping exposures at 1/3 dose. This translates any abrupt stitching error into a small but uniform change in the line-to-space ratio of the grating. The phase mask was used with the double-exposure photoprinting technique [K. O. Hill, F. Bilodeau, B. Malo, T. Kitagawa, S. Thériault, D. C. Johnson, J. Albert, and K. Takiguchi, *Opt. Lett.* **19**, 1314 (1994)]: a KrF excimer laser holographically imprints an apodized chirped Bragg grating in a hydrogen loaded SMF-28 optical fiber. Our experiments have demonstrated a spectral delay of -1311 ps/nm with a linearity of ± 10 ps over the 3 dB bandwidth of the resonant wavelength of the FBG. The reflectance, centered on 1550 nm, shows a side-lobe suppression of -25 dB. Fabrication processes and optical characterization will be discussed. © 1998 American Vacuum Society. [S0734-211X(98)06406-3]

I. INTRODUCTION

High-bit-rate long haul fiber optic transmission systems, which incorporate erbium-doped fiber amplifiers and standard telecommunications fiber, suffer from chromatic dispersion of ~ 17 ps/(nm km). Chirped fiber Bragg gratings (CFBG) have proven to be viable devices to compensate this chromatic dispersion.¹

An example of pulse degradation is shown in Fig. 1. This simulation shows a 50 ps input pulse and an output pulse after 200 km propagation.² In order to restore this degraded pulse, an element with an equal and opposite dispersion is needed. Figure 2 shows a schematic representation of a compensation system. In this example, a CFBG could be used in reflection mode to provide 0.5 ns compensation.

CFBGs can be fabricated by using zero-order-nulled phase masks^{1,3,4} or be fabricated holographically.^{5,6} Ideally the spectral delay characteristic of a CFBG should have a linear response. There are, however, ripples or deviations from linearity in the phase delay response that can impact system performance. These nonlinearities arise from a number of factors, namely phase errors in electron-beam fabri-

cated phase masks,⁶ imperfect apodization,⁵ and nonuniformity of the fiber and ultraviolet (UV) irradiation^{7,8} process.

In this work, we investigate a novel *e*-beam writing technique in order to minimize phase errors. Six and ten cm chirped zero-order-nulled phase masks were fabricated using this method. The phase mask and the double-exposure photoprinting technique¹ were then used to create a partially apodized CFBG device suitable for compensation of fiber dispersion over a single 100 GHz bandwidth channel.

II. FABRICATION

The mask fabrication employed electron beam lithography and reactive ion etching (RIE). A 6-in.-diam quartz disk was spun with 300 nm of ZEP-520 resist (a nonchemically amplified copolymer of chloromethacrylate and methylstyrene) and baked at 170 °C for one hour. Since this is a chromeless mask, it is necessary to thermally evaporate an Au overlayer for charge dissipation during the *e*-beam exposure.

The nanolithography was performed using a Leica VB6 electron-beam system. The exposure conditions were 9 nA probe current, 50 keV acceleration potential, 300 $\mu\text{m} \times 300$ μm field, 5 nm pixel, and 25 MHz stepping speed. The sub-

^{a)}Electronic mail: tiberio@cnf.cornell.edu

^{b)}Present address IBM Research Center, Yorktown Heights, NY.

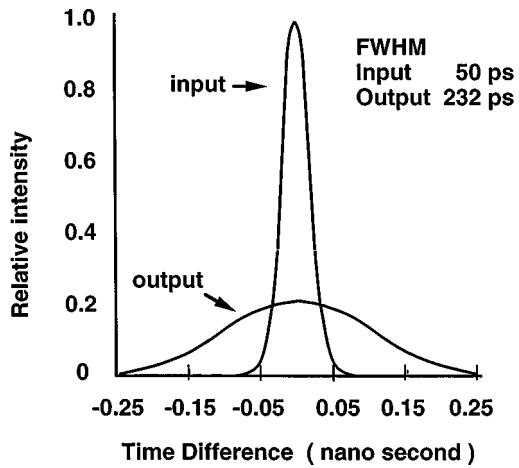


FIG. 1. Simulation of 50 ps input pulse and output pulse shape after propagating through 200 km of single mode fiber with dispersion of 16 ps/(nm km).

strate stage has a 150 mm motion and is monitored by a $\lambda/1024$ laser interferometer. The exposure dosage was $90 \mu\text{C}/\text{cm}^2$.

After the gold conduction layer was stripped by wet etching, the ZEP-520 resist was developed in xylenes for 120 s. The resist image was transferred into the quartz disk by RIE. The etching conditions were 2.0 Pa pressure, $0.17 \text{ W}/\text{cm}^2$ power density, with CF_4 and H_2 gases (42 and 5 sccm, respectively). These parameters yield an etch rate selectivity of SiO_2 to resist greater than 2:1. The desired etch depth for zeroth order cancellation is 248 nm. Large area etch monitors were unacceptable for the determination of the etch depth. Instead the disk was removed from the etcher and small adjacent grating sections were measured using atomic force microscopy (AFM). Etching was continued until the target depth was reached.

Figure 3 shows AFM images of the resulting gratings. Images show smooth etched surfaces and good etch depth uniformity. At present conventional pyramidal probes are used, so the AFM is used to determine the etch depth and scanning electron microscopy is used to measure the line to space ratio. Sharpened ‘‘super tips’’ will be used in the future.

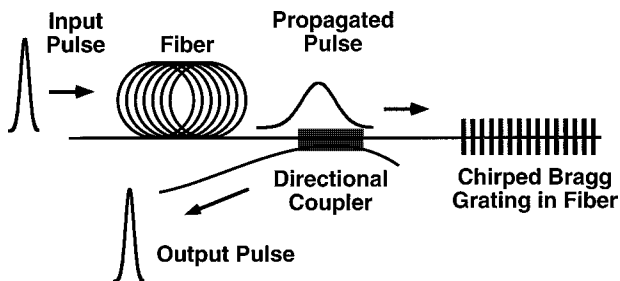


FIG. 2. Schematic of dispersion compensation using chirped fiber Bragg grating.

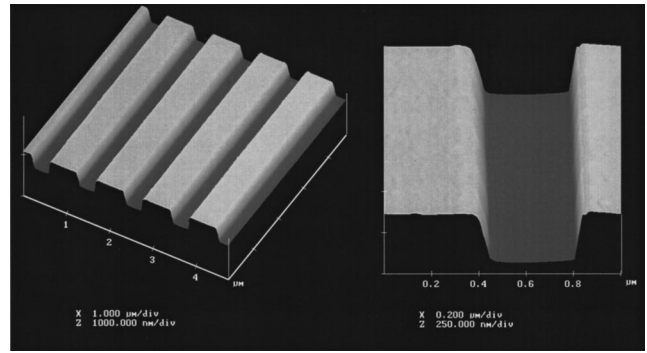


FIG. 3. Atomic force micrograph of quartz phase mask grating. Loop I=0 to 1000, Scaling=fixed+(0.514 ppm×I), Move relative X=100 μm , Y=0 μm , Expose pattern, end loop.

III. CONTROL PROGRAM

Previous work in grating lasers have demonstrated precision pitch control. An array of distributed Bragg reflector lasers, with adjacent laser grating periods differing by 0.5 nm was reported.⁹ Also distributed feedback (DFB) lasers with grating periods differing by 0.28 nm were reported.¹⁰ These laser arrays used deflection field stretching to accomplish the fine pitch control for 10 to 20 discrete wavelengths. Our present experiments expand on that previous work. In our CFBG fabrication, a precise bandwidth was chosen and *all* wavelengths within the band need to be exposed.

This linear increase, chirp, in the grating period, is only 0.55 nm over the 10 cm grating. This is too small to be defined by computer aided design and a digital deflection system. Instead, the chirp was incorporated by repeatedly rescaling the analog electronics used for field size calibration. A portion of the exposure program is shown in Fig. 4. This seemingly simple program demonstrates the flexibility and precision control of the grating exposure that is possible using electron beam lithography:

- (1) As will be discussed later, a 100 μm stage motion was used to expose the 10 cm grating, hence the number of iterations is set to 1000.
- (2) The computer aided design (CAD) pattern has a digitally defined period of 1070 nm. The lower limit of the grating period, 1070.11 nm, was achieved by scaling the pattern by the ‘‘fixed’’ coefficient.
- (3) The ratio of the periods, 1070.66 and 1070.11 nm, is 514 ppm. This chirp slope and the longer wavelength limit are given by the scaling coefficient, in this example 0.514 parts per million.
- (4) In addition to the deflection, the individual stage moves must also be stretched by the scaling command. In order

```

Loop I = 0 to 1000
Scaling = Fixed + (0.514 ppm × I)
Move Relative ΔX=100 μm, ΔY=0 μm
Expose Pattern
end loop
    
```

FIG. 4. Electron beam control program for linearly chirped grating exposure.

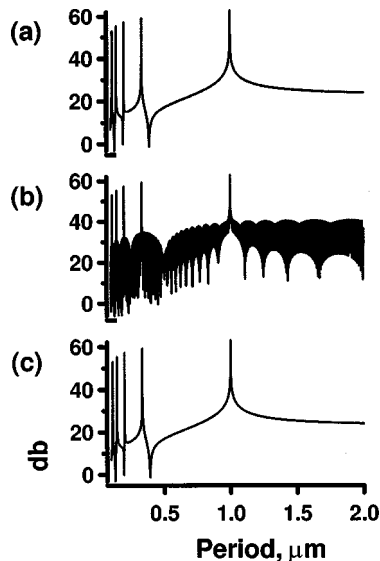


FIG. 5. Spatial FFT of simulated gratings: (a) ideal grating, (b) “tiled” grating with 20 nm stitching errors, (c) averaged grating with 20 nm stitching errors.

to correctly account for the accumulation of scaled stage moves, a move-relative-to-current-position command is used.

Although this example is for a linearly chirped 10 cm grating, arbitrarily shaped functional forms, up to 15 cm in length, are also possible.

IV. STITCHING TECHNIQUE

Special attention must be paid to minimize any field stitching and exposure artifacts. This was done by using overlapping fields in a “voting” or “averaging” method. Rather than expose in a step-and-repeat fashion with abutted deflection fields and stage motion, each line of the grating was exposed by the accumulation of partial exposures. For example, the exposure was performed using a 300 μm pat-

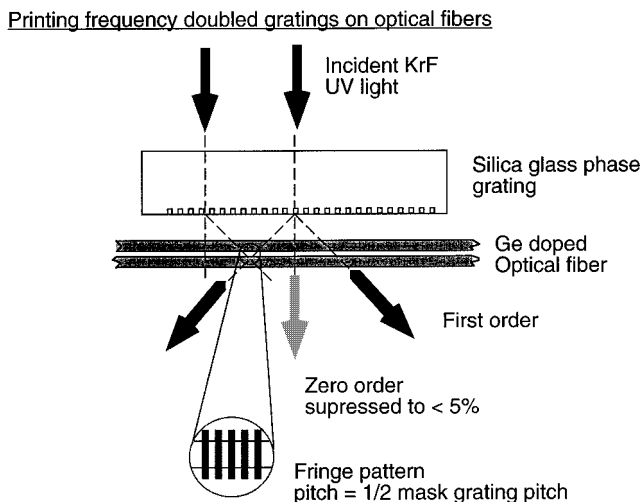


FIG. 6. Schematic of holographic exposure.

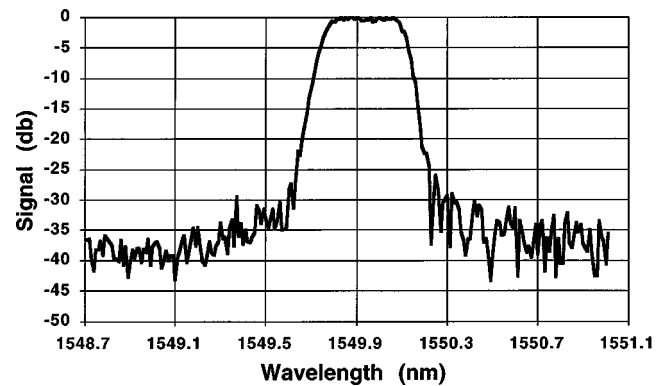


FIG. 7. Spectral reflectance of chirped fiber Bragg grating.

tern and exposure field size, with only a 100 μm stage motion. As a result each grating line is exposed by the accumulation of three overlapping exposures at 1/3 of a dose. Each line of the grating is exposed by a rightward, a centered, and a leftward deflected beam. This translates any stitching error into a small but uniform change in the line-to-space ratio of the grating. The resulting grating is uniform without abrupt phase errors.

Previous multiple-pass grating investigations have included: scanning electron microscopy (SEM) inspection of the gratings and resulting Moiré patterns; comparison of the grating duty cycles; and pulsed laser spectroscopy of passive waveguides. All three experiments indicated uniform gratings with no detectable phase errors.¹¹

Simulations were run to compare exposure techniques. The longitudinal axis was defined as 0.1 nm exposure elements (excels). The simulated exposure assumed the resist to be very high contrast with a critical dose 30% of nominal exposure. Each excel of a 1 mm grating was simulated to be exposed by an ideal uniform deflection field; by a “butted” deflection field with a 20 nm magnification error and by the “three pass averaging” technique. A fast Fourier transform (FFT) of the resulting grating was taken. Figure 5 shows the spatial Fourier components of an ideal grating with no *e*-beam writing errors; a grating with an abrupt magnification error of 20 nm at each of 100 writing fields; a grating with the same 20 nm magnification errors but exposed using the averaging technique. The simulation clearly shows the benefit of averaging. As anticipated, the averaging technique moves the high frequency errors into the low frequency (long spatial period) regime. The effects of random placement errors will be address in the future.

V. FIBER GRATING AND OPTICAL RESULTS

The phase mask was then used to holographically expose a fiber Bragg grating (FBG) into the core of a standard Ge-doped telecommunications fiber.¹² Using the double-exposure photoimprinting technique with the phase mask,¹ a KrF excimer laser was used to imprint a partially apodized chirped Bragg grating in a hydrogen loaded SMF-28 single mode optical fiber (Fig. 6). A super-Gaussian apodization function was used. The Bragg resonance of the grating was

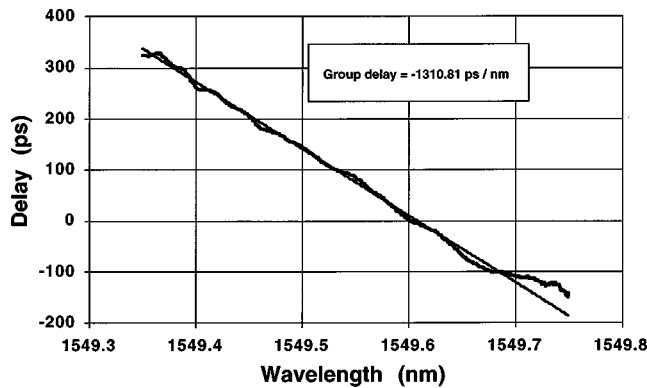


FIG. 8. Phase delay vs wavelength.

centered at 1550 nm, and shows a side-lobe suppression of -25 dB while measured in reflection (Fig. 7). Using a dispersion measurement technique described previously,¹³ our experiments have demonstrated a spectral delay of -1311 ps/nm with deviations from linear time delay of ± 10 ps over the 3 dB bandwidth of the resonant wavelength of the FBG (Fig. 8). This time delay ripple approaches the ± 8.5 ps ripple obtained from a CFBG device fabricated with a stitch-error free holographically written phase mask.¹⁴ Further optimization of the UV exposure and apodization techniques are in progress.

VI. CONCLUSION

Electron beam lithography and reactive ion etching were used to produce a zero-order-nulled phase mask. The grating period was varied from 1070.11 to 1070.66 nm. Using this phase mask, a CFBG device suitable for compensation of fiber dispersion over a single channel was created with a low

group delay ripple of ± 10 ps. The quality of the device is comparable to those fabricated with stitch-error free holographically exposed phase masks.

ACKNOWLEDGMENTS

This work was performed in part at the Communication Research Center and in part at the Cornell Nanofabrication Facility which is supported by the National Science Foundation under Grant No. ECS-9319005, Cornell University, and industrial affiliates.

- ¹K. O. Hill, F. Bilodeau, B. Malo, T. Kitagawa, S. Thériault, D. C. Johnson, J. Albert, and K. Takiguchi, *Opt. Lett.* **19**, 1314 (1994).
- ²Adapted from Specview, ElectroPhotonics Corp.
- ³M. Durkin, M. Ibsen, M. J. Cole, and R. I. Laming, *Electron. Lett.* **33**, 1891 (1997).
- ⁴D. Garthe, G. Milner, and Y. Cai, *Electron. Lett.* **34**, 582 (1998).
- ⁵M. C. Farries, K. Sugden, D. C. J. Reid, I. Bennion, A. Molony, and M. J. Goodwin, *Electron. Lett.* **30**, 891 (1994).
- ⁶R. Stubbe, B. Sahlgren, S. Sandgren, and A. Asseh, OSA Topical Meeting, Portland, Oregon, Sept. 9–11, post deadline paper PD1, 1995.
- ⁷J. Albert, S. Thériault, F. Bilodeau, D. C. Johnson, K. O. Hill, P. Sixt, and M. J. Rooks, *IEEE Photonics Technol. Lett.* **8**, 1334 (1996).
- ⁸F. Ouellette, OSA Topical Meeting, Williamsburg, Virginia, Oct. 26–28, Paper BMG13, 1997.
- ⁹R. C. Tiberio and R. J. Lang, *J. Vac. Sci. Technol. B* **9**, 2842 (1991).
- ¹⁰D. M. Tennant, K. F. Dreyer, K. Feder, R. P. Gnall, T. L. Koch, U. Koren, B. I. Miller, C. Vartuli, and M. G. Young, *J. Vac. Sci. Technol. B* **12**, 3689 (1994).
- ¹¹R. C. Tiberio, R. D. Martin, and R. J. Lang, *J. Vac. Sci. Technol. B* **12**, 3746 (1994).
- ¹²K. O. Hill, F. Bilodeau, D. C. Johnson, and J. Albert, *Appl. Phys. Lett.* **62**, 1035 (1993).
- ¹³S. Ryu, Y. Horiuchi, and K. Mochizuki, *J. Lightwave Technol.* **7**, 1177 (1989).
- ¹⁴S. J. Mihailov, F. Bilodeau, K. O. Hill, D. C. Johnson, J. Albert, D. Stryckman, and C. Shu, *Proceedings of the 24th European Conference on Optical Communications ECOC '98* (1998), Vol. 1, P. 283.